Effect of Operating Conditions of a Double-Drum Vibratory Roller on Vehicle Vide Comfort

Le Van Quynh[1], Nguyen Thi Kim Thoa[2]

[1,2]*Faculty of Automotive and Power Machinery Engineering, Thai Nguyen University of Technology, Thai Nguyen, Vietnam*

---***---

Abstract - *In order to analyze the effect of the operating conditions of a double-drum vibratory roller on vehicle ride comfort, a half-vehicle ride dynamic model is established based on the drum-ground interactions for simulation and evaluation. The effects of the different vehicle operating conditions on vehicle ride comfort including road surfaces, the low and high excitation frequencies for the drums are analyzed in this study. The weighted r.m.s acceleration responses of the vertical driver's seat (a_{ws}) and pitch angle of the cab (a_{wphi}) according to the ISO 2631:1997(E) standard are chosen as objective functions. The results show that the effect of the road surface roughness on vehicle ride comfort is very obvious. Especially, when the vehicle changing road surface condition moves from the good road surface condition (class B) to average road surface condition (class C) and then to very to poor road surface condition (class D), the a_{ws} and a_{wphi} values increase from 79.95 %, 97,43% and 79.94 %, 43,97%. The vehicle ride comfort is significantly improved when vehicle compacts at the high excitation frequency.*

Key Words: Vibratory roller, double-drum, operating condition, Ride comfort

1. INTRODUCTION

The vibratory roller operates and moves on various kinds of soil ground. The vibration excitation sources causing vehicle's body vibration are not only the excitations of the interaction between wheel and deformation ground soil but also are the ones of vibration drum and the engine which is one of the main reasons for the driver fatigue. The influence of vehicle operating conditions on vehicle ride comfort as well road surface friendliness was very obvious [1]. The various operating conditions were selected for evaluating the acceleration-frequency characteristics of the suspension system of the heavy vehicles [2]. The influence of the different operating conditions on the driver ride comfort of a single –drum vibratory roller was analyzed by a 3D nonlinear dynamic model [3]. The deformed ground conditions such as the dry sand and clay ground surfaces were selected to find out the effects of design parameters of cab's isolation system on vibratory roller ride comfort [4]. The deformed ground conditions were selected to compare with experimental results of a single-drum vibratory roller[20].

In order to investigate the effects of design parameters of the isolation system on vibratory roller ride comfort, the design parameters of drum's metal rubber isolation system of tandem vibratory roller on ride comfort were analyzed by using tandem vibratory roller dynamic model with 7 degrees of freedom(DOF)[5]. The effects of cab's various isolation systems of a single-drum vibratory roller on vehicle ride comfort were figured out by using vehicle lumped-parameter model with three different cab's isolation mounts[6]. The design parameters of the isolation systems and the various operating conditions of a single-drum vibratory roller were evaluated to see the effects on vehicle ride comfort[7].

In order to improve to vehicle ride comfort, the design parameters of drum's isolation systems of a double-drum vibrating roller were reviewed and optimized using the genetic algorithm (GA) [8]. The optimal design parameters of cab's isolation systems of a single-drum vibrating roller were found out by a multi-objective genetic algorithm[9]. The design parameters of cab's main isolation system[10] and cab's auxiliary isolation system[11] were optimized by using the finite element method (FEM), and the cab shaking of vibratory rollers was controller using the horizontal auxiliary damping mount[12]. Drum's isolation system of vibratory road roller was controlled based on Magneto-Rheological semi-active damper[13] and the combined control method of Fuzzy and PID control was proposed to control the cab isolation system of soil compactor based on the non-linear vehicle dynamic model[14].

In this study, a half-vehicle ride dynamic model of a double-drum vibratory roller is established for analyzing and evaluating the effect of the operating conditions of a double-drum vibratory roller on vehicle ride comfort. The weighted r.m.s acceleration responses of the vertical driver's seat (a_{ws}) and pitch angle of the cab (a_{wphi}) according to the ISO 2631:1997(E) [15] standard are chosen as objective functions. The effect of the different vehicle operating conditions on vehicle ride comfort including road surfaces, the excitation frequencies such as the low and high excitation frequencies for the drums are analyzed based on the objective functions. Matlab/simulink software is used to simulate the vehicle dynamic models and calculate the objective functions.

2. HALF-VEHICLE RIDE DYNAMIC MODEL

A double- double drum vibratory roller with the isolation systems of double drums, cab's isolation system and seat suspension system is selected for analyzing the various operating conditions. A half-vehicle ride dynamic model is established based on the drum-ground interactions as shown in Fig-1.

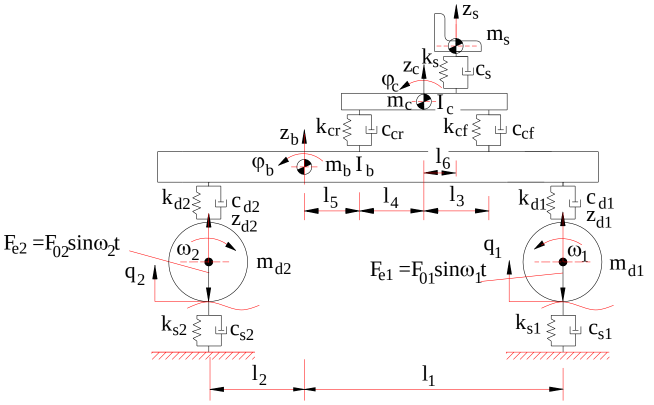

Fig-1: Half-vehicle ride dynamic model

In Fig-1, m_{d1}, m_{d2}, m_b, m_c and m_s are the mass of the front and rear vibrating drums, vehicle body, cab and driver's seat, respectively; I_b and I_c are the moment of inertia of the vehicle body and cab; k_s and c_s are the stiffness and damping coefficients of driver's seat suspension system; k_{cf}, k_{cr} and c_f, c_r are the stiffness and damping coefficients of the front and rear cab's isolation systems, respectively; k_{di} and c_{di} are the stiffness and damping coefficients of front and rear drums, respectively; z_{di}, z_b, z_c and z_s are the vertical displacements at centre of gravity of the drums, vehicle body, cab and driver's seat, respectively; φ_b and φ_c are the pitch angle displacements of the vehicle body and cab, respectively; and q_{di} are the front and rear excitation of road surface roughnesses, respectively; l_j, are the distances; $F_{e1}=F_{01}sin(\omega_1 t)$ and $F_{e2}=F_{02}sin(\omega_2 t)$ are the force excitations of the front and rear vibrating drums; F_{0i} are the amplitudes of the front and rear force excitations; ω_i are the angular frequencies of the front and rear vibrators; (i=1÷2, j=1÷6).

The equations of motion for a double-drum vibrating roller using Newton's second law of motion are written in two operating conditions below[8].

Vehicle moves into the workshop: Vehicle wheel contacts and moves on types of road or ground surfaces such as rigid, flexible, soft, etc[20]. The drum of vibratory roller in contact with the rigid road surface is the contact point which is considered in this study. From the half-vehicle ride dynamic model, as shown in Fig. 1, the motion equations of vehicle mass are written as follows:

$$m_s\ddot{z}_s = k_s\left(z_s - z_c - l_6\varphi_c\right) + c_s\left(\dot{z}_s - \dot{z}_c - l_6\dot{\varphi}_c\right) \quad (1)$$

$$\begin{aligned} m_c\ddot{z}_c &= \left[k_s\left(z_s - z_c - l_6\varphi_c\right) + c_s\left(\dot{z}_s - \dot{z}_c - l_6\dot{\varphi}_c\right)\right] \\ &-\left[k_{cf}\left(z_c + l_3\varphi_c - z_b - l_5\varphi_b\right) + c_{cf}\left(\dot{z}_c + l_3\dot{\varphi}_c - \dot{z}_b - l_5\dot{\varphi}_b\right)\right] \\ &-\left[k_{cr}\left(z_c - l_4\varphi_c - z_b - \left(l_3+l_4+l_5\right)\varphi_b\right) + c_{cr}\left(\dot{z}_c - l_4\dot{\varphi}_c - \dot{z}_b - \left(l_3+l_4+l_5\right)\dot{\varphi}_b\right)\right] \end{aligned} \quad (2)$$

$$\begin{aligned} I_c\varphi_c &= \left[k_s\left(z_s - z_c - l_6\varphi_c\right) + c_s\left(\dot{z}_s - \dot{z}_c - l_6\dot{\varphi}_c\right)\right]l_6 \\ &-\left[k_{cf}\left(z_c + l_3\varphi_c - z_b - l_5\varphi_b\right) + c_{cf}\left(\dot{z}_c + l_3\dot{\varphi}_c - \dot{z}_b - l_5\dot{\varphi}_b\right)\right]l_3 \\ &+\left[k_{cr}\left(z_c - l_4\varphi_c - z_b - \left(l_3+l_4+l_5\right)\varphi_b\right) + c_{cr}\left(\dot{z}_c - l_4\dot{\varphi}_c - \dot{z}_b - \left(l_3+l_4+l_5\right)\dot{\varphi}_b\right)\right]l_4 \end{aligned} \quad (3)$$

$$\begin{aligned} m_b\ddot{z}_b &= \left[k_{cf}\left(z_c + l_3\varphi_c - z_b - l_5\varphi_b\right) + c_{cf}\left(\dot{z}_c + l_3\dot{\varphi}_c - \dot{z}_b - l_5\dot{\varphi}_b\right)\right] \\ &+\left[k_{cr}\left(z_c - l_4\varphi_c - z_b - \left(l_3+l_4+l_5\right)\varphi_b\right) + c_{cr}\left(\dot{z}_c - l_4\dot{\varphi}_c - \dot{z}_b - \left(l_3+l_4+l_5\right)\dot{\varphi}_b\right)\right] \\ &-\left[k_{d1}\left(z_b + l_1\varphi_b - q_1\right) + c_s\left(\dot{z}_b + l_1\dot{\varphi}_b - \dot{q}_1\right)\right] \\ &-\left[k_{d2}\left(z_b - l_2\varphi_b - q_2\right) + c_s\left(\dot{z}_b - l_2\dot{\varphi}_b - \dot{q}_2\right)\right] \end{aligned} \quad (4)$$

$$\begin{aligned} I_b\ddot{\varphi}_b &= \left[k_{cf}\left(z_c + l_3\varphi_c - z_b - l_5\varphi_b\right) + c_{cf}\left(\dot{z}_c + l_3\dot{\varphi}_c - \dot{z}_b - l_5\dot{\varphi}_b\right)\right]\left(l_3+l_4+l_5\right) \\ &+\left[k_{cr}\left(z_c - l_4\varphi_c - z_b - \left(l_3+l_4+l_5\right)\varphi_b\right) + c_{cr}\left(\dot{z}_c - l_4\dot{\varphi}_c - \dot{z}_b - \left(l_3+l_4+l_5\right)\dot{\varphi}_b\right)\right]l_5 \\ &-\left[k_{d1}\left(z_b + l_1\varphi_b - q_1\right) + c_s\left(\dot{z}_b + l_1\dot{\varphi}_b - \dot{q}_1\right)\right]l_1 \\ &+\left[k_{d2}\left(z_b - l_2\varphi_b - q_2\right) + c_s\left(\dot{z}_b - l_2\dot{\varphi}_b - \dot{q}_2\right)\right]l_2 \end{aligned} \quad (5)$$

Vehicle operates in the workshop: When vehicle works and compresses on many different types of properties of deformable ground soil such as the hysteretic force – deflection properties, the elasto-plastic properties, etc. The properties of deformable ground soil are linear by the stiffness and damping coefficients of the elastic soil ground. From the half-vehicle ride dynamic model as shown in Fig. 1, the motion equations of the front drum mass, rear drum mass and vehicle body mass are written as follows:

$$\begin{aligned} m_b\ddot{z}_b &= \left[k_{cf}\left(z_c + l_3\varphi_c - z_b - l_5\varphi_b\right) + c_{cf}\left(\dot{z}_c + l_3\dot{\varphi}_c - \dot{z}_b - l_5\dot{\varphi}_b\right)\right] \\ &+\left[k_{cr}\left(z_c - l_4\varphi_c - z_b - \left(l_3+l_4+l_5\right)\varphi_b\right) + c_{cr}\left(\dot{z}_c - l_4\dot{\varphi}_c - \dot{z}_b - \left(l_3+l_4+l_5\right)\dot{\varphi}_b\right)\right] \\ &-\left[k_{d1}\left(z_b + l_1\varphi_b - z_{d1}\right) + c_s\left(\dot{z}_b + l_1\dot{\varphi}_b - \dot{z}_{d1}\right)\right] \\ &-\left[k_{d2}\left(z_b - l_2\varphi_b - z_{d2}\right) + c_s\left(\dot{z}_b - l_2\dot{\varphi}_b - \dot{z}_{d2}\right)\right] \end{aligned} \quad (6)$$

$$\begin{aligned} I_b\ddot{\varphi}_b &= \left[k_{cf}\left(z_c + l_3\varphi_c - z_b - l_5\varphi_b\right) + c_{cf}\left(\dot{z}_c + l_3\dot{\varphi}_c - \dot{z}_b - l_5\dot{\varphi}_b\right)\right]\left(l_3+l_4+l_5\right) \\ &+\left[k_{cr}\left(z_c - l_4\varphi_c - z_b - \left(l_3+l_4+l_5\right)\varphi_b\right) + c_{cr}\left(\dot{z}_c - l_4\dot{\varphi}_c - \dot{z}_b - \left(l_3+l_4+l_5\right)\dot{\varphi}_b\right)\right]l_5 \\ &-\left[k_{d1}\left(z_b + l_1\varphi_b - z_{d1}\right) + c_s\left(\dot{z}_b + l_1\dot{\varphi}_b - \dot{z}_{d1}\right)\right]l_1 \\ &+\left[k_{d2}\left(z_b - l_2\varphi_b - z_{d2}\right) + c_s\left(\dot{z}_b - l_2\dot{\varphi}_b - \dot{z}_{d2}\right)\right]l_2 \end{aligned} \quad (7)$$

$$\begin{aligned} m_{d1}\ddot{z}_{d1} &= F_{01}\sin\omega_1 t + \left[k_{d1}\left(z_b + l_1\varphi_b - z_{d1}\right) + c_s\left(\dot{z}_b + l_1\dot{\varphi}_b - \dot{z}_{d1}\right)\right] \\ &-\left[k_{s1}z_{d1} + c_{d1}\dot{z}_{d1}\right] \end{aligned} \quad (8)$$

$$\begin{aligned} m_{d2}\ddot{z}_{d2} &= F_{02}\sin\omega_2 t + \left[k_{d2}\left(z_b - l_2\varphi_b - z_{d2}\right) + c_s\left(\dot{z}_b - l_2\dot{\varphi}_b - \dot{z}_{d2}\right)\right] \\ &-\left[k_{s2}z_{d2} + c_{d2}\dot{z}_{d2}\right] \end{aligned} \quad (9)$$

The rigid road surface roughnesses[17]: the road surface roughness is simulated according to the International Standards Organization (ISO) 8608 [15]. A road surface roughness is usually assumed to be a zero-mean stationary Gaussian random process and can be generated through an inverse Fourier transformation based on a power spectral density (PSD) function [14]. The road surface roughness is generated as the sum of a series of harmonics:

$$q(t)=\sum_{k=1}^{N}\sqrt{2G_q(n_{mid-k})\Delta n_k}.\cos(2\pi n_{mid-k}t+\phi_k) \quad (10)$$

where, the spatial frequency range, $n_1<n<n_2$, is divided into several uniform intervals which have a width of Δn_k; $G_q(n)$ is PSD function (m^3/cycle/m) for the road surface elevation, the power density $G_q(n)$ in every small interval is substituted by $Gq(n_{mid-k})$, where n_{mid-k} (k= 1, 2,..., n) is center frequency among its intervals; n_k is the wave number (cycle/m); ϕ_k is the random phase uniformly distributed from 0 to 2π.

The rigid road surface with ISO class C (Average) according to the standard ISO 8068 is shown in Fig-2.

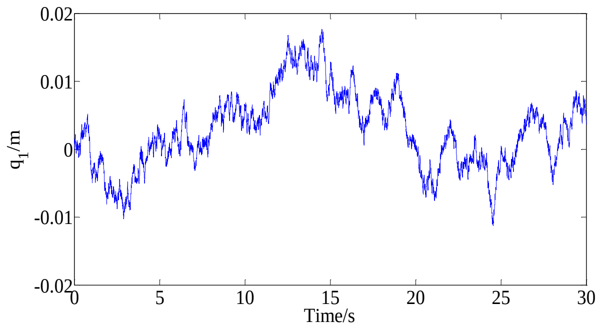

Fig- 2: Road surface roughness ISO class C according to ISO 8068.

3 VEHICLE RIDE COMFORT CRITERIA[4],[5],[18]

The vehicle ride comfort is evaluated based on ISO 2631-1 (1997) [15], the vibration evaluation based on the basic evaluation method including measurements of the weighted root-mean-square (r.m.s.) acceleration is defined as

$$a_w=\left[\frac{1}{T}\int_0^T a_w^2(t)dt\right]^{1/2} \quad (11)$$

In this formula, $a_w(t)$ is the weighted acceleration (translational and rotational) as a function of time, m/s^2; T is the duration of the measurement, s.

For indications of likely reactions to various magnitudes of overall vibration in the public transport and vehicle, a synthetic index-called weighted r.m.s acceleration, a_w can be calculated from formula Eq.(11); besides, the r.m.s. value of the acceleration in vehicle would be compared with the values in Table-1.

Table- 1: Comfort levels related to a_w threshold values

$a_w/(m.s^2)$	Comfort level
< 0.315	Not uncomfortable
0.315÷0.63	A little uncomfortable
0.5 ÷ 1.0	Fairly uncomfortable
0.8 ÷ 1.6	Uncomfortable
1.25 ÷ 2.5	Very uncomfortable
> 2	Extremely uncomfortable

4. RESULTS AND DISCUSSION

In order to solve the general dynamic differential equation for a double-drum vibratory roller which is presented in section 2 for analyzing and evaluating the effect of vehicle operating conditions on vehicle ride comfort. Matlab/Simulink software is used with a specific set of parameters of vehicle[19] to stimulate and define the objective function when vehicle operates under two different conditions.

Vehicle moves into the workshop: Effect of road surface roughness

In order to analyze the effect of the road surface roughness on ride comfort of a double-drum vibratory roller when vehicle moves into the workshop with a velocity of 15km/h, four road surface conditions from class A (very good) to class D (poor) in ISO/TC 80686 have been considered as inputs to the vehicle-road coupled model.

The simulation results of the time domain acceleration responses of the vertical driver's seat (a_s) and pitch angle of the cab(a_{phi}) when vehicle moves the ISO road surface class C and v=15km/h are shown in Fig.3.

From the results of the acceleration responses, we could determine the values of the weighted r.m.s acceleration of the vertical driver's seat (a_{ws}) and pitch angle of the cab (a_{wphi}) when vehicle moves on the various road conditions, as shown in Tab.2. Tab.2 shows that the a_{ws} and a_{wphi} values increase quickly when vehicle moves on the poor road surface conditions, which makes the negative effects on vehicle ride comfort. Especially, when the vehicle moves on the good road surface condition (class B) to average road surface condition (class C) and then to very to poor road surface condition (class D), the a_{ws} and a_{wphi} values increase from 79.95 %, 97,43% and 79.94 %, 43,97%. Those values of a_{ws} and a_{wphi} are extremely uncomfortable conditions for driver comfort according to ISO 2631-1 (1997) with the comfort levels related to a_w threshold values in Tab.1 when vehicle moves on the various road conditions.

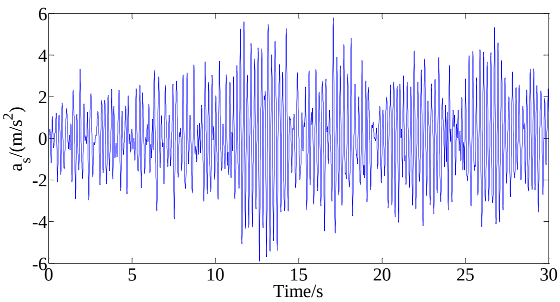

(a) Vertical driver's seat (a_s)

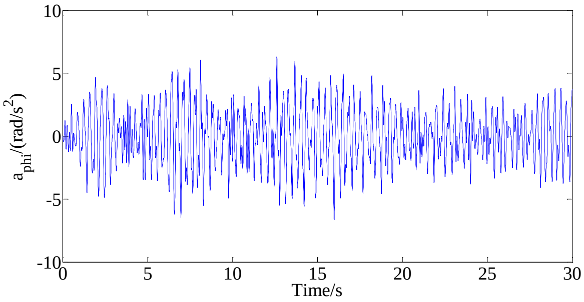

(b) Pitch angle of the cab(a_{phi})

Fig- 3: Time domain acceleration responses when vehicle moves with a velocity of 15km/h

Table- 2: a_{ws} and a_{wphi} values with four road conditions

Values / Conditions	$a_{ws}/(m.s^2)$	$a_{wphi}/(rad.s^2)$
ISO class A	0.3187	0.6178
ISO class B	1.0641	1.2089
ISO class C	1.9148	2.1753
ISO class D	3.7803	3.1753

Vehicle operates in the workshop: Effect of road surface roughness

In order to analyze the effect of the various compression conditions on vehicle ride comfort when vehicle compacts on original place, the low and high excitation frequencies for drums are selected for analysis. When vehicle compacts on original place at the low excitation frequency (F_{01}=128000N và f_1=48Hz and F_{02}=0 và f_2=54Hz) for front drum, the simulation results of the time domain acceleration responses of the vertical driver's seat (a_s) and pitch angle of the cab(a_{phi}) are shown in Fig.4

Similarly, from the results of the acceleration responses, we could determine the values of the weighted r.m.s acceleration of the vertical driver's seat (a_{ws}) and pitch angle of the cab (a_{wphi}) when vehicle compacts at the various excitation frequency conditions for drums, as shown in Tab.3. Tab.3 shows that the a_{ws} and a_{wphi} values increase quickly when vehicle compacts on original place at low excitation frequency, making the negative effects on vehicle ride comfort. The a_{ws} and a_{wphi} values with the high excitation frequency for rear drum reduce by 10.73% and 66.28% in comparison with the low excitation frequency for front drum. The vehicle ride comfort is significantly improved when vehicle compacts at the high excitation frequency. Those values of a_{ws} and a_{wphi} are comfortable conditions for driver comfort according to ISO 2631-1 (1997) with the comfort levels related to a_w threshold values in Tab.1 when vehicle compacts at the various excitation frequency conditions for drums.

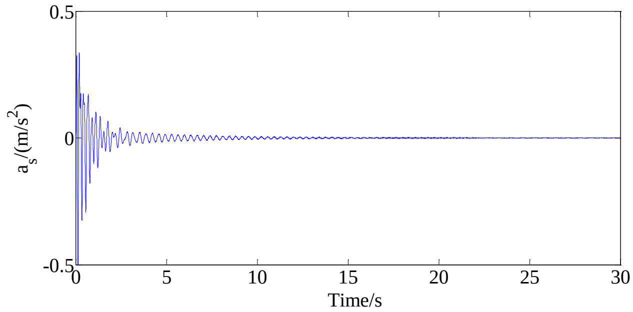

(a) Vertical driver's seat (a_s)

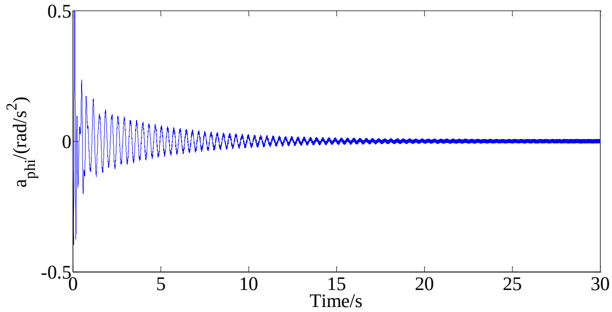

(b) Pitch angle of the cab(a_{phi})

Fig- 4: Time domain acceleration responses when vehicle compacts on original place at the low excitation frequency

Similarly, from the results of the acceleration responses, we could determine the values of the weighted r.m.s acceleration of the vertical driver's seat (a_{ws}) and pitch angle of the cab (a_{wphi}) when vehicle compacts at the various excitation frequency conditions for drums, as shown in Tab.3.

Table- 3: a_{ws} and a_{wphi} values with the various excitation frequency conditions for drums

Values / Conditions	$a_{ws}/(m.s^2)$	$a_{wphi}/(rad.s^2)$
f_1=48Hz and f_2=0 Hz	0.0373	0.0429
f_1=0Hz and f_2=54 Hz	0.0177	0.0258
f_1=48Hz and f_2=54 Hz	0.0420	0.0210

5. CONCLUSIONS

In this study, a half-vehicle ride dynamic mode based on the drum-ground interactions is established to analyze the effects of the different vehicle operating conditions on vehicle ride comfort. The major conclusions can be drawn from the analysis and evaluation results as follows:

i) The a_{ws} and a_{wphi} values increase quickly when vehicle moves on the poor road surface conditions, making the negative effects on vehicle ride comfort. Especially, when the vehicle changing road surface condition moves on the good road surface condition (class B) to average road surface condition (class C) and then to very to poor road surface condition (class D), the a_{ws} and a_{wphi} values increase from 79.95 %, 97,43% and 79.94 %, 43,97%.

ii) The a_{ws} and a_{wphi} values with the high excitation frequency for rear drum reduce by 10.73% and 66.28% in comparison with the low excitation frequency for front drum. The vehicle ride comfort is significantly improved when vehicle compacts at the high excitation frequency.

iii) The analytical results of this paper can provide theoretical basis for the isolation system design of the vibrating rollers.

Acknowledgment

This research was supported financially by Thai Nguyen University of Technology, TNUT, Viet Nam.

REFERENCES

[1] Van Quynh, L.(2017). "Influence of semi-trailer truck operating conditions on road surface friendliness", Vibroengineering PROCEDIA 16, p.67–72.

[2] V Nguyen, V Le, R Jiao, H Yuan(2020). "Low-frequency vibration analysis of heavy vehicle suspension system under various operating conditions", Mathematical Models in Engineering, Vol. 6, Issue 1, p. 13-22.

[3] Quynh Le Van (2013). "Vibration Study and Control Cab of Vibratory Roller". Southeast University, Nanjing, China.

[4] Le Van Quynh, Thao V. T. P., et al (2019). "Influence of design parameters of cab's isolation system on vibratory roller ride comfort under the deformed ground surfaces". International Research Journal of Engineering and Technology (IRJET), Vol. 6, Issue 6, p. 1974-1978.

[5] Le Van Quynh, Thao V. T. P., et al(2019). "Study on influence of design parameters of drum's metal rubber isolation system of double vibratory roller on ride comfort", International Research Journal of Engineering and Technology (IRJET), Vol. 6, Issue 6, p. 1647-1651.

[6] Liem N. V., Run Z. J., et al(2018). "Vibration analysis and modeling of an off-road vibratory roller equipped with three different cab's isolation mounts" Shock and Vibration, Vol. 2018, p. 8527574.

[7] Kordestani Rakheja, et al (2010). "Analysis of ride vibration environment of soil compactors", SAE International Journal of Commercial Vehicles, Vol. 3, Issue 1, p. 259-272.

[8] LV Quynh, VTP Thao, TT Phong(2020). "Optimal design parameters of drum's isolation system for a double-drum vibratory roller", Vibroengineering PROCEDIA, Vol. 31 , p. 74-79.

[9] Le V. Q., Nguyen K. T. (2018). "Optimal design parameters of cab's isolation system for vibratory roller using a multi-objective genetic algorithm". Applied Mechanics and Materials, Vol. 875, p. 105-112

[10] LV Quynh, Z Jianrun, et al(2020). "Experimental modal analysis and optimal design of cab's isolation system for a single drum vibratory roller", Vibroengineering PROCEDIA, Vol. 31, p. 52-56.

[11] Quynh L. V., Zhang J. R., et al (2011) "Vibration analysis and optimal design for cab's isolation system of vibratory roller". Advanced Materials Research, Vol. 199, 200, p. 936-940.

[12] V Nguyen, R Jiao,et al (2020). "Study to control the cab shaking of vibratory rollers using the horizontal auxiliary damping mount", Mathematical Models in Engineering, Vol. 6, Issue 1, p. 57-65.

[13] Liu S. N., Yan S. R., et al(2012). "Dynamic and control of vibratory road roller based on Magneto-Rheological semi-active damper", Advanced Materials Research, Vol. 479, Issue 481, p. 1200-1204.

[14] V Nguyen, R Jiao, V Le, A Hoang. "Performance of PID-Fuzzy control for cab isolation mounts of soil compactors", Mathematical Models in Engineering, Vol. 5, Issue 4, 2019, p. 137-145.

[15] .ISO 2631-1 (1997). Mechanical Vibration and Shock-Evaluation of Human Exposure to Whole-Body Vibration, Part I: General Requirements. The International Organization for Standardization, 1997.

[16] ISO 8068 (1995). Mechanical Vibration-Road Surface Profiles-Reporting of Measured Data. International Organization for Standardization.

[17] HA Tan, LV Quynh, NV Liem, BV Cuong, LX Long (2019). "Influence of damping coefficient into engine rubber mounting system on vehicle ride comfort", Vibroengineering PROCEDIA, Vol. 29, p. 112-117

[18] Le Xuan Long, Le Van Quynh, Bui Van Cuong (2018), "Study on the influence of bus suspension parameters on ride comfort", Vibroengineering PROCEDIA, Vol. 21, p. 77-82.

[19] Doan Thanh Binh. Study on controlling a cab's semi-active isolation system for a construction machine. Master of Science thesis: Thai Nguyen University of Technology. Thai Nguyen, Viet Nam, 2019.

[20] Le V. (2017). Ride Comfort Analysis of Vibratory Roller via Numerical Simulation and Experiment. DEStech Transactions on Engineering and Technology Research.